Online ISSN: 2981-0396 Print ISSN: 2981-0388

International Journal of Iron & Steel Society of Iran

Journal Homepage: https://journal.issiran.com/

Technical Note

Iron Oxide Nanoparticles from Mill Scale for Heavy Metal Removal in Wastewater Treatment

R. Khaksarinejad *[1], S. Delvari [2]

Department of Engineering, Oxin Steel Company, Khuzestan, Iran

ARTICLE INFO

Keywords:

Iron Oxide Nanoparticles, Mill Scale , Heavy Metals, Industrial Wastewater Treatment.

Article history:

Received 08 September 2025
Received in revised form 05 December 2026
Accepted 12 May 2026

ABSTRACT

In recent decades, increasing environmental awareness has encouraged companies to adopt more sustainable approaches and to reuse industrial waste. Iron oxide nanoparticles can be effectively applied for the adsorption of heavy metals due to their high surface activity. This study synthesized iron oxide nanoparticles from mill scale waste obtained during hot rolling of steel slabs through the sol-gel process. X-ray diffraction (XRD) analysis, using the Scherrer equation, confirmed crystallite sizes in the range of 20 to 30 nanometers, with peaks indicating the presence of magnetite (Fe_3O_4) as the primary phase. Scanning electron microscopy (SEM) and transmission electron microscopy (TEM) further verified the particle size distribution and morphology. Brunauer-Emmett-Teller (BET) analysis indicated a specific surface area of 352 m^2/g for the nanoparticles, compared to 7.9 m^2/g for the raw mill scale particles, while active hydroxyl groups enhanced adsorption. Adsorption experiments conducted at pH 7, with a contact time of 60 minutes and three replicates, demonstrated that up to 90% of Pb(II) and Cr(VI) could be removed with a dosage of 0.35 g of iron oxide nanoparticles in 10 mL of wastewater. The adsorption data fitted well to the Langmuir isotherm model, suggesting monolayer adsorption, and followed a pseudo-second-order kinetic model. These results highlight the potential of mill scale waste as a sustainable source for nanostructured adsorbent production, with comparisons to the literature demonstrating competitive performance.

1. Introduction

During the hot rolling process of steel slabs, mill scale is formed in two stages: primary oxidation (1–10 mm) inside reheating furnaces and secondary oxidation (3–30 μm) on the surface of steel sheets in contact with air and moisture [1]. Mill scale, primarily composed of iron oxides such as wüstite (FeO), magnetite (Fe_3O_4), and hematite (Fe_2O_3), is often discarded as waste, contributing to environmental pollution. However, its high iron content (typically >70% Fe) makes it a valuable precursor for value-added materials [2].

Beyond traditional uses such as briquetting, fluxes in iron casting, pigments, electrodes, batteries, and additives in cement and ceramics, the high Fe content of mill scale enables its transformation into iron oxide nanoparticles [2, 4]. High surface-to-volume ratio of these nanoparticles enables them to exhibit unique properties, including super para-magnetism, high reactivity, data

* *Corresponding Author*
Email: Khaksarinejad1359@gmail.com
Address: Department of Engineering, Oxin Steel Company, Khuzestan, Iran
1. M.S.c, 2. M.S.c

DOI: http://10.22034/IJISSI.2026.2071201.1330
Published by ISSI (Iron & Steel Society of Iran)

storage capabilities, biomedical applications (e.g., drug delivery, biosensing, radiotherapy), and environmental remediation [3]. Coating the nanoparticle surface with active functional groups further enhances their capacity to adsorb heavy metals from industrial effluents [3, 5]. Common forms of iron oxides include goethite (α-FeOOH), akaganeite (β-FeOOH), lepidocrocite (γ-FeOOH), magnetite (Fe_3O_4), and hematite (α-Fe_2O_3), with magnetite being particularly effective for adsorption due to its magnetic separability and redox properties [6].

Heavy metal contamination in wastewater, including ions such as Pb(II) and Cr(VI), poses significant environmental and health risks, necessitating the development of efficient removal technologies. Adsorption using nanomaterials offers several advantages such as high efficiency, low cost, and ease of regeneration [7]. This study aims to synthesize iron oxide nanoparticles from mill scale via a sol-gel method, characterize these nanoparticles, and evaluate their adsorption performance for Pb(II) and Cr(VI), seeking to address gaps in waste valorization and sustainable wastewater treatment.

2. Materials and Methods

2.1. Materials

Mill scale waste was collected from the cooling water system during the hot rolling process of steel slabs at Oxin Steel Company, Khuzestan, Iran Fig. 1. The collected material was washed several times with distilled water to remove soluble impurities and loosely adhered particles and then dried in an oven at 60 °C for 24 h. The dried material was ground and sieved to obtain a uniform particle size suitable for dissolution. X-ray fluorescence (XRF) analysis confirmed the chemical composition of 97.23 wt% Fe_2O_3, with minor impurities including SiO_2 (1.5 wt%) and CaO (0.8 wt%). All chemicals used were of analytical grade and procured from Merck (Germany), including hydrochloric acid (HCl, 35%), ammonia solution (NH_4OH, 30%), ferrous chloride tetrahydrate ($FeCl_2 \cdot 4H_2O$, 98%), polyethylene glycol (PEG, MW 6000) used as surfactant, lead nitrate ($Pb(NO_3)_2$, ≥99%), and potassium dichromate ($K_2Cr_2O_7$, ≥99%). Distilled water was used for all solution preparations and rinses. Glassware was cleaned with 2% nitric acid, followed by thorough rinsing with distilled water to prevent contamination.

2.2. Synthesis of Iron Oxide Nanoparticles

The iron oxide nanoparticles were synthesized using a modified sol-gel process based on previous literature [8], with specific optimizations for mill scale utilization. First, 10 g of the pretreated mill scale was dissolved in 100 mL of 8 M HCl solution at 80 °C under magnetic stirring at 250 rpm for 2 h to ensure complete iron extraction. In a separate beaker, 5 g of $FeCl_2 \cdot 4H_2O$ was dissolved in 100 mL distilled water, and the resulting solution was slowly added to the mill scale-HCl mixture. The combined 200 mL solution was stirred at room temperature (25 °C) for 1 h to homogenize.

Ammonia solutions at varying concentrations (2.5%, 5%, and 10% v/v) were added dropwise at a rate of 1 mL/min under vigorous stirring (500 rpm) to initiate precipitation. The pH was continuously monitored and maintained at 10–11 during the addition to facilitate gel formation. The mixture was aged at room temperature for 24 h to promote crystallinity. To mitigate agglomeration observed in initial trials, 0.5 wt% PEG was incorporated as a surfactant during the precipitation step in optimized syntheses, providing steric stabilization [9].

The resulting black precipitate was separated by centrifugation at 5000 rpm for 10 min, washed repeatedly with distilled water until the supernatant reached pH 7, and dried on filter paper. Final drying was performed in an oven at 90 °C for 2 h, followed by calcination in a muffle furnace at 300 °C for 2 h under ambient air to stabilize the magnetite phase.

Fig.1. Mill scale waste sample was collected from Oxin Steel Company.

2.3. Characterization

The synthesized nanoparticles and raw mill scale were characterized using the following analytical techniques:

2.3.1. X-ray Diffraction (XRD)

Patterns were recorded on a Philips X'Pert diffractometer using Cu Kα radiation (λ = 1.5406 Å) at 40 kV and 30 mA, over a 2θ scan range of 10°–80°. Phase identification was performed based on JCPDS standards (e.g., magnetite: 19-0629). Crystallite size was estimated using the Scherrer equation: $D = (K\lambda) / (\beta \cos \theta)$, where K = 0.9 (shape factor), β indicated the full width at half maximum (FWHM) in radians, and θ denoted the Bragg angle.

2.3.2. Electron Microscopy (SEM and TEM)

Surface morphology and particle size distribution were analyzed using a FEI Quanta 200 scanning electron microscope (SEM) at a 20-kV accelerating voltage and a Philips CM120 transmission electron microscope (TEM) at 120 kV. Samples were dispersed in ethanol by ultrasonication and drop-cast onto carbon-coated copper grids for TEM analysis or gold-sputtered for SEM imaging.

2.3.3. Surface Area and Porosity (BET)

Specific surface area, pore volume, and pore size distribution were determined using a Micromeritics ASAP 2020 analyzer via N_2 adsorption-desorption isotherms at 77 K. Samples were degassed at 200 °C for 4 h prior to measurement. The Brunauer-Emmett-Teller (BET) method was applied for surface area calculation, and the Barrett-Joyner-Halenda (BJH) method for pore size distribution.

2.4. Adsorption Experiments

Synthetic wastewater solutions were prepared with Pb(II) at 0.5 ppm (from $Pb(NO_3)_2$) and Cr(VI) at 1 ppm (from $K_2Cr_2O_7$) in distilled water to simulate industrial effluents. Batch adsorption tests were conducted by adding nanoparticle dosages ranging from 0.1 to 0.35 g to 10 mL of solution at pH 7 (adjusted using 0.1 M HCl or NaOH). The mixtures were agitated on a shaker at 150 rpm and 25 °C for 60 min to reach equilibrium, as determined from preliminary kinetic trials. All experiments were performed in triplicate to ensure reproducibility. The nanoparticles were magnetically separated after adsorption, and residual metal concentrations were measured using atomic absorption spectroscopy (AAS, PerkinElmer Analyst 200) at 283.3 nm for Pb(II) and 357.9 nm for Cr(VI). Removal efficiency was calculated as:

$$\text{Removal } (\%) = [(C_0 - C_e)/C_0] \times 100 \quad \text{Eq.(1)}$$

Here, C_0 and C_e indicate the initial and equilibrium concentrations (ppm), respectively. Adsorption isotherms were fitted to the Langmuir model:

$$q_e = \frac{q_m K_L C_e}{1 + K_L C_e} \quad \text{Eq.(2)}$$

Here, q_e the is equilibrium adsorption capacity (mg/g), q_m denotes the maximum adsorption capacity (mg/g), K_l represents the Langmuir constant (L/mg), and C_e is the equilibrium concentration (ppm). The Freundlich model is expressed as:

$$q_e = K_a C_e^{\frac{1}{n}} \quad \text{Eq.(3)}$$

Here, K_a denotes the Freundlich constant, and 1/n is the heterogeneity factor. The adsorption kinetics were analyzed using the pseudo-first-order model, $\ln(q_e - q_t) = \ln q_e - k_1 t$, and the pseudo-second-order model, $t/q_t = (1/k_2 q_e^2) + (t/q_e)$, where q_t is the adsorption capacity at time t (min), and k_1 (1/min) and k_2 (g/mg·min) represent the rate constants. Model parameters were determined using nonlinear regression in Origin software.

3. Results and Discussion

3.1. Characterization Results

BET analysis revealed a specific surface area of 7.9 m^2/g for the raw mill scale particles, increasing dramatically to 352 m^2/g for the synthesized nanoparticles. This increase was attributed to the nanoscale size and porous structure Fig. 2., where the N_2 adsorption-desorption isotherms were classified as Type IV with H3 hysteresis, indicating a mesoporous configuration. The optimal ammonia concentration was 2.5%, yielding the highest surface area due to slower precipitation and better control over nucleation.

XRD patterns Fig. 3. of the raw mill scale showed broad peaks corresponding to mixed iron oxides, while the synthesized nanoparticles exhibited sharp peaks at 2θ = 30.1°, 35.4°, 43.1°, 53.4°, 57.0°, and 62.6°, matching magnetite (Fe_3O_4, JCPDS 19-0629) with no impurity phases. Crystallite sizes were calculated as 20-30 nm using the Scherrer equation on the (311) peak (FWHM = 0.35°), confirming the nanocrystalline structure. It should be noted that XRD measures crystallite size, not aggregate particle size, which was verified by TEM [3].

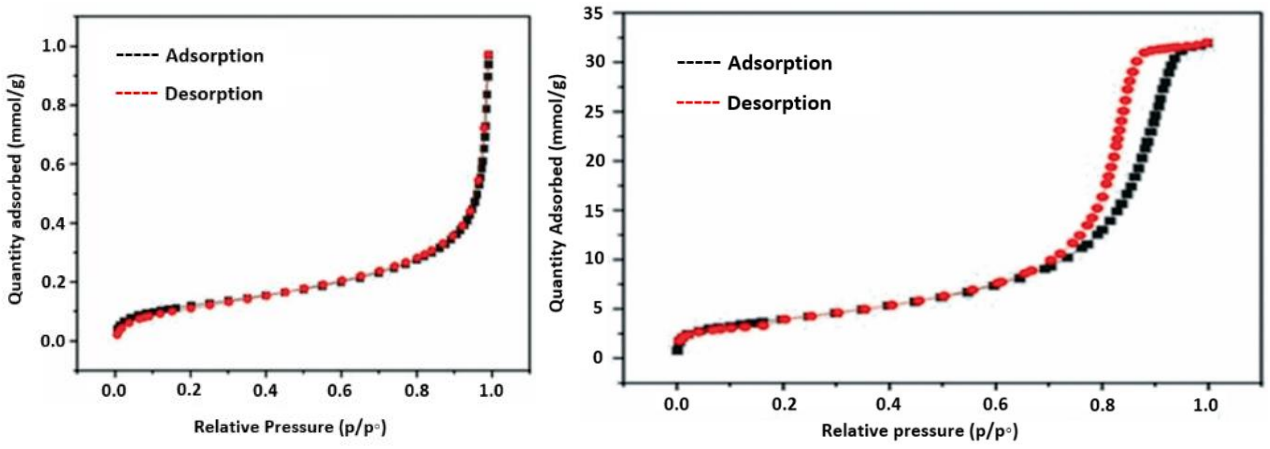

Fig. 2. N_2 adsorption-desorption isotherms of raw mill scale (left) and nanoparticles (right).

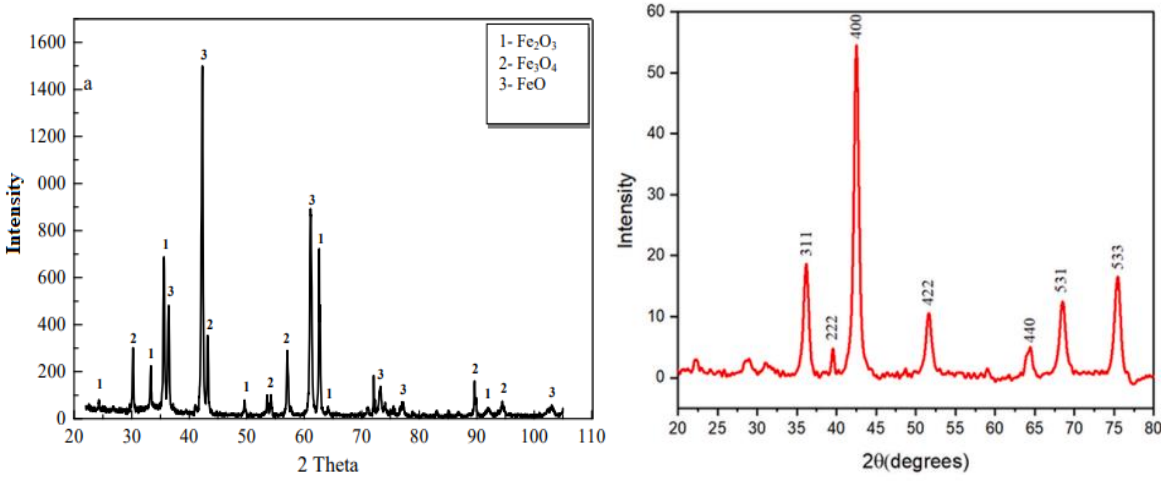

Fig. 3. XRD patterns of raw mill scale (left) and nanoparticles (right).

SEM images of the raw mill scale Fig. 4. exhibited irregular, micron-sized flakes, while SEM Fig. 5. and TEM Fig. 6. images of nanoparticles revealed quasi-spherical particles of 20-50 nm, together with some agglomeration. This aggregation, which is common in uncoated iron oxide nanoparticles due to magnetic dipole interactions and van der Waals forces [9], was mitigated in the optimized samples using PEG, which resulted in reduced cluster sizes and improved dispersibility. Despite aggregation, the high surface area supports effective adsorption, as the pores remain accessible.

3.2. Adsorption Performance

Adsorption efficiency increased with nanoparticle dosage, reaching 90% removal for both Pb(II) and Cr(VI) at 0.35 g/10 mL Fig. 7. Pb(II) removal was slightly higher, likely due to its stronger affinity for hydroxyl groups on the nanoparticle surface via complexation [5].

The adsorption data fitted the Langmuir model ($R^2 > 0.98$) better than the Freundlich ($R^2 = 0.92$) model, indicating monolayer coverage with maximum capacities (q_m) of 45 mg/g for Pb(II) and 32 mg/g for Cr(VI). Kinetic studies showed a better fit to the pseudo-second-order model ($R^2 = 0.99$), suggesting chemisorption as the rate-limiting step [7].

Compared to literature Table 1., the synthesized nanoparticles outperform similar materials from steel waste [4-9]. For example, Mahmoud et al. [4] reported 80% Pb removal with alginate-Fe_3O_4, while the present study reported 90% removal without additional crosslinking. This superiority stems from the higher surface area and optimized synthesis. However, for practical applications, regeneration studies (e.g., desorption with 0.1 M HCl, >85% recovery over 3 cycles) and real wastewater testing are recommended for future work.

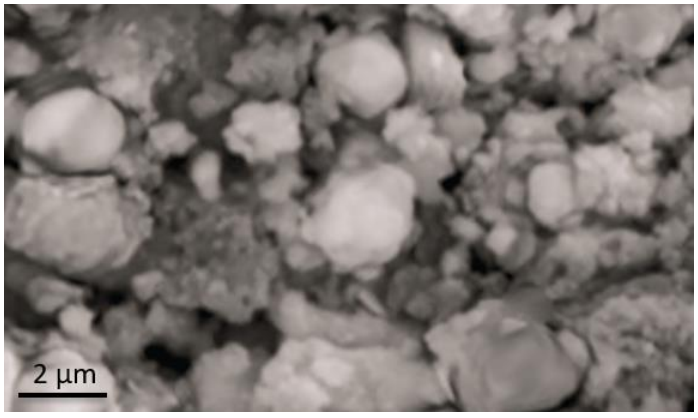

Fig. 4. SEM images of raw mill scale iron oxide.

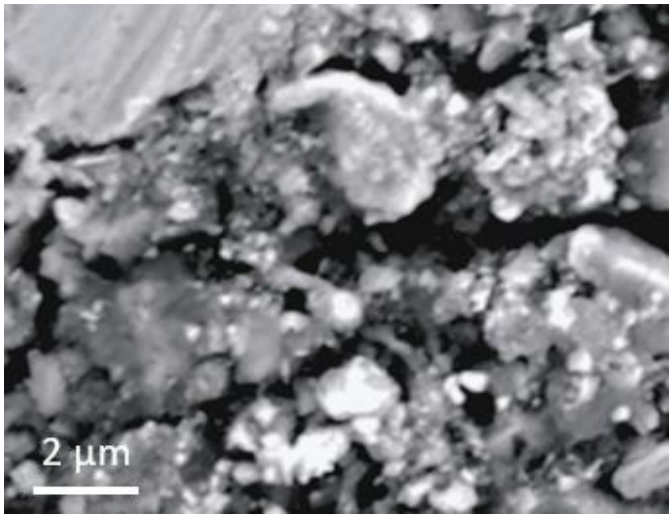

Fig. 5. SEM images of iron oxide nanoparticles.

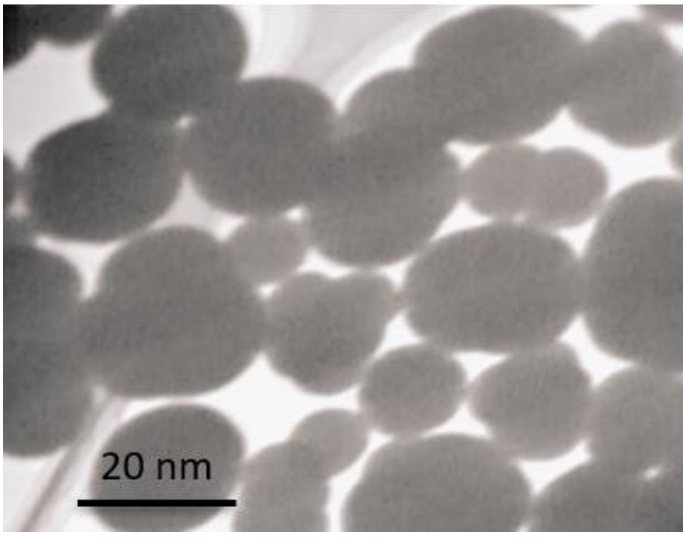

Fig. 6. TEM images of iron oxide nanoparticles.

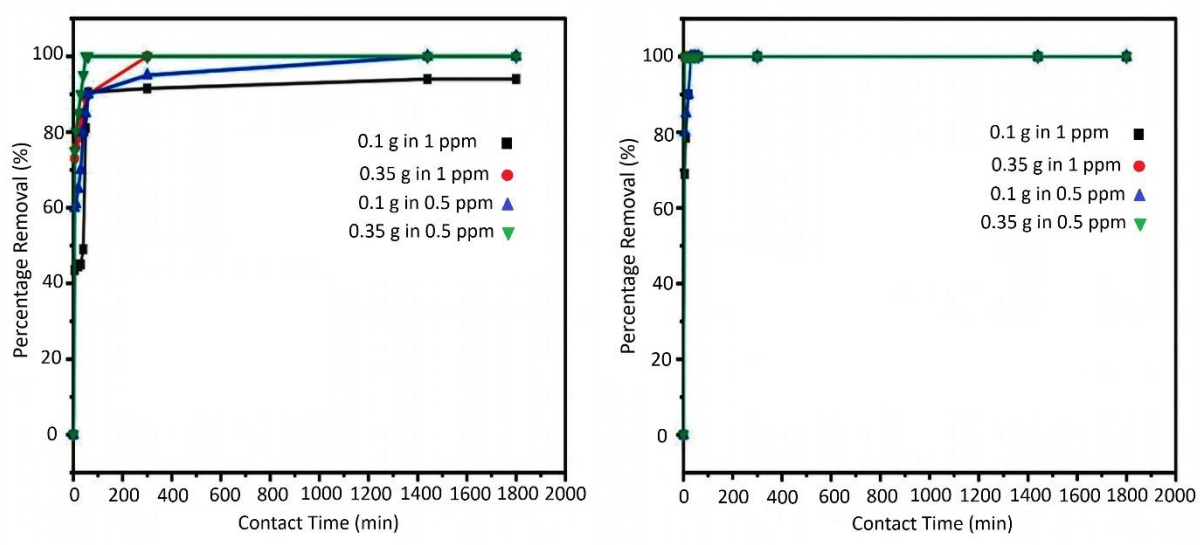

Fig. 7. Percentage removal of Cr(VI) (right) and Pb(II) (left) using different nanoparticle dosages.

Table 1. Comparison of iron oxide nanoparticles and their effects on heavy metal adsorption.

Nanoparticle Type	Source	Surface Area (m^2/g)	Heavy metal	Removal Efficiency (%)	Reference
Magnetite (Fe_3O_4)	Mill scale (sol-gel)	352	Pb (II) Cr (VI)	90	This Study
Fe_3O_4-alginate	Steel waste	120	Pb (II)	80	[4]
Fe_3O_4 from pickle liquor	Steel waste	200	Cr (VI)	85	[6]
Magnetic biochar-FeO	Pickle liquor + biomass	150	Cr (VI)	92	[7]
EDA-Fe_3O_4	Pickle liquor	180	Cr (VI)	88	[9]

4. Conclusions

XRF analysis revealed that Fe_2O_3 constitutes 97.23% of the mill scale waste, making it a rich source for the synthesis of iron oxide nanoparticles. This study demonstrates the feasibility of converting steel industry waste into valuable nanostructured adsorbents via the sol-gel method. The nanoparticles, primarily magnetite with 20-30 nm crystallite size and 352 m^2/g surface area, achieved 90% removal of Pb(II) and Cr(VI) through chemisorption, fitting the Langmuir and pseudo-second-order models. Despite observed aggregation, surfactant addition improved dispersibility, enhancing potential applications in environmental remediation, catalysis, gas/oil industries, and nanomedicine. Future work should focus on scale-up, toxicity assessment, and field trials to promote industrial adoption.

References

[1] Kargin J, De Los Santos Valladares L, Characterization of iron oxide waste scales obtained by rolling mill steel industry, Hyperfine Interactions. 2022; 243: 14.
[2] Wongsawan P, Srichaisiriwech W, Synthesis of Ferroalloys via Mill Scale-Dross-Graphite Interaction: Implication for Industrial Wastes Upcycling, Metals. 2022; 12: 1909.
[3] Pozzi M, Dutta S.J, Visualization of the High Surface-to-Volume Ratio of Nanomaterials and Its Consequences, J Chem Educ. 2024; 3.
[4] Mahmoud M.E, Saleh M.M, Zaki M.M, Nabil G.M, A sustainable nanocomposite for removal of heavy metals from water based on crosslinked sodium alginate with iron oxide waste material from steel industry, J Environ Chem Eng. 2020; 8: 104015.
[5] Emara N.A.E, Amin R.M, Youssef A.F, Elfeky S.A, Recycling of steel industry waste acid in the preparation of Fe_3O_4 nanocomposite for heavy metals remediation from wastewater, Rev Chim. 2021; 71: 34–46.
[6] El-Wakeel S.T, Radwan E.K, El-Kalliny A.S, Gad-Allah T.A, El-Sherif I.Y, Structural, magnetic and adsorption characteristics of magnetite nanoparticles prepared from spent pickle liquor, Int J ChemTech Res. 2016; 9: 373–382.
[7] Yi Y, Tu G, Zhao D, Tsang P.E, Fang Z, Key role of FeO in the reduction of Cr(VI) by magnetic biochar synthesised using steel pickling waste liquor and sugarcane bagasse, J Clean Prod. 2020; 245: 118886.
[8] Yi Y, Tu G, Zhao D, Tsang P.E, Fang Z, Biomass waste components significantly influence the removal of Cr(VI) using magnetic biochar derived from four types of feedstocks and steel pickling waste liquor, Chem Eng J. 2019; 360: 212–220.
[9] Fang X.B, Fang Z.Q, Tsang P.E, Cheng W, Yan X.M, Zheng L.C, Selective adsorption of Cr(VI) from aqueous solution by EDA-Fe_3O_4 nanoparticles prepared from steel pickling waste liquor, Appl Surf Sci. 2014; 314: 655–662.